Soliton Boundstates in Dimerized Spin Chains

Erik S. Sørensen[1], Ian Affleck[2], David Augier[1], and Didier Poilblanc[1]

[1] Laboratoire de Physique Quantique & UMR CNRS 5626, Université Paul Sabatier, 31062 Toulouse, France
[2] Department of Physics and Astronomy, and Canadian Institute for Advanced Research, University of British Columbia, Vancouver, BC, V6T 1Z1, Canada

1 Introduction

In the beginning of the eighties Faddeev and Takhtajan [1] suggested that the fundamental excitations of the one-dimensional Heisenberg model should be viewed as massless kink-like $s = 1/2$ objects, the so called spinons. Although this is not the only way to think of the excitations in the Heisenberg model it is often a quite useful picture. A natural generalization of the Heisenberg model is to include a next-nearest neighbor term $\mathbf{S}_i \cdot \mathbf{S}_{i+2}$ of strength J_2, resulting in the following Hamiltonian:

$$H = \sum_i [J\mathbf{S}_i \cdot \mathbf{S}_{i+1} + J_2\mathbf{S}_i \cdot \mathbf{S}_{i+2}], \tag{1}$$

Several physical compounds exists that are fairly well described by such a Hamiltonian. Perhaps most notably $CuGeO_3$ [2]. It is in this case useful to think of the spins as being arranged in a zig-zag manner as shown in Fig. 1. At the critical coupling $J_{2c} \simeq 0.241167$ [3–5] systems described by

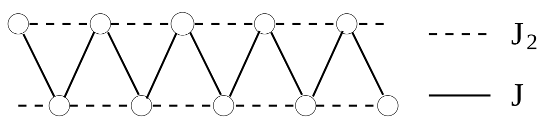

Fig. 1. The zig-zag chain

the Hamiltonian, Eq. 1, enters a spontaneously dimerized phase and a gap opens up in the excitation spectrum. The Majumdar-Ghosh [6] (MG) point, $J_2 = J/2$, constitutes a disorder point [7] beyond which the short-range correlations become incommensurate. The associated Lifschitz point, where the peak in the structure factor moves away from π, has been determined to be $J_2/J = 0.52063(6)$ [8] using DMRG methods and the ensuing short-range incommensurate correlations have been studied in detail by White and Affleck [9]. In the present contribution we focus on how the behavior of the spinons is changed once the dimerized phase is entered. The fundamental excitations are now real kinks separating two different dimerization patterns and we therefore refer to them as solitons. These solitons become massive in the dimerized phase.

In order to take into account the three-dimensional lattice in a one-dimensional model one often introduces an explicit dimerization δ yielding a staggered nearest neighbor coupling:

$$H = \sum_i [J(1 + \delta(-1)^i)\mathbf{S}_i \cdot \mathbf{S}_{i+1} + J_2 \mathbf{S}_i \cdot \mathbf{S}_{i+2}]. \tag{2}$$

The phase diagram of this model as well as the correlations have previously been investigated using DMRG techniques by Pati et al. [10] and Chitra et al. [11]. Schönfeld et al. [12] have investigated the magnetic field phase diagram using DMRG methods and the thermodynamics of related models have been investigated using transfer matrix DMRG by Maisinger et al. [13]. Our interest here is to study the spectrum of low lying excitations in the dimerized phase, $J_2 > J_{2c}$, to show that solitons and anti-solitons form a ladder of triplet-singlet bound-states [14].

A solitonic picture of the excitations in frustrated spin chains was first introduced by Shastry and Sutherland [15] and more recently by Khomskii et al. [16] as well as others [17–20]. In the context of the so called saw-tooth lattice or delta-chain, corresponding to Fig. 1 with every second J_2 coupling set to zero, the solitonic excitations have been investigated by Nakamura et al. [21] and Sen et al. [22]. In this case the symmetry between solitons and anti-solitons is absent. Thermodynamic properties of this model has been investigated using transfer matrix DMRG methods by Maisinger et al. [13].

2 Numerical Considerations

In order to study the excitations in the dimerized phase we have performed extensive DMRG calculations. See the contribution by Noack and White in this book. However, where needed we use exact diagonalization techniques to obtain a more complete picture of the excitation spectrum. For the model Eq. 1 the ground-state (and a few excited states) are exactly known at the MG point. In the vicinity of the MG point the correlations of the above models are extremely short-ranged and DMRG calculations are exact for the matrix product ground-state of the Hamiltonian, Eq. 1, at the MG point. For a discussion of matrix product states see the contribution of Rommer in this volume. The short correlation length is very helpful when performing numerical work since finite size corrections will be very small and for the exact diagonalization results we are essentially limited to the neighborhood of the MG point if we want to study the excitations in detail. The short correlation length also improves the precision of the DMRG calculations tremendously and we usually never have to keep more than $m = 128$ states. In order to study the excitations it is however crucial that we can distinguish odd and even multiplets. This is done by performing the calculations in the $S^z_T = \sum_i S^z_i = 0$ subspace and using spin-inversion as a symmetry along with real-space parity. Both of these symmetries reduces the size of the Hilbert space by roughly a factor of two and hence combining them reduces the overall computational over-head by a factor of four. Spin-inversion has the added benefit of being an 'on-site' symmetry and can therefore also be used in combination with the finite system method. Under spin-inversion even and odd total spin multiplets transform differently and can be distinguished. Symmetries are extensively used in DMRG calculations and for more details we refer the reader to the contributions by Ramasesha and Barford in the present volume. A simple way of implementing parity in the infinite system method is discussed in Ref. [23] and there is a nice paper by Ramasesha et al, Ref. [24], where the implementation of more complicated symmetries are discussed.

3 The Soliton Gap

We begin with a discussion of systems without any explicit dimerization, described by Eq. 1. For a system with an even number of spins the ground-state is always a singlet. However, for an odd number of spins the lowest energy state has spin $\frac{1}{2}$. We therefore say that the odd-site system contains one soliton. One way of defining the energy, Δ_{sol}, required to create a soliton is therefore to say that it is equal to $\Delta_{sol} = \lim_{n\to\infty} E_0(L=2n+1)-(2n+1)e_0$, where $E_0(2n+1)$ is the ground-state energy of an odd-length system with $L=2n+1$ sites, and e_0 is some measure of the ground-state energy per spin of the corresponding even-length system. Here it is crucial that periodic boundary conditions are used. Similar ideas have been used by Malék et al. [19]. At the MG point the ground-state energy for even-length systems is $-3LJ/8$, hence $e_0=-3J/8$ does not depend on L. Thus, using exact diagonalization techniques, we have obtained $\Delta_{sol}/J = 0.1168,\ J_2 = J/2$. If the soliton does

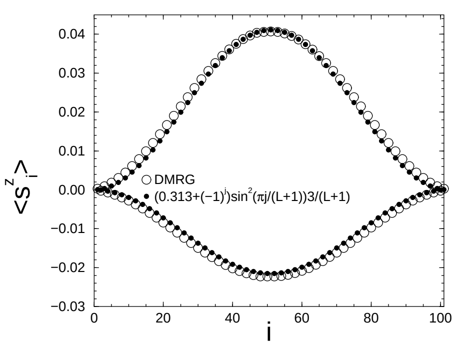

Fig. 2. $< S_i^z >$ as a function of i. DMRG results are shown for L=101, with $S^z_{tot} = 1/2$, $m = 128$. Clearly the soliton is repelled by the open ends and enters approximately a particle in a box state $< S_i^z > \simeq [\text{const} + (-1)^i \sin^2(\pi i/(L+1))]$ indicated by the solid circles.

not interact with the chain boundaries we can check this result using DMRG calculations on systems with open boundary conditions. This turns out to be the case and DMRG results for the soliton gap is in complete agreement with the above result. However, the fact that the soliton remains a 'bulk' excitation is non-trivial. In Fig. 2 the ground-state spin-density is shown for an odd-length system. Clearly, the soliton is repelled by the open boundaries and enters roughly a particle in a box state as indicated by the solid circles. If the density of solitons can be increased sufficiently the spin-density should be experimentally observable in NMR experiments. Away from the MG point finite-size corrections to Δ_{sol} become much more important and a reliable determination is only possible using DMRG calculations. As a function of J_2 we have calculated the soliton gap (Ref. [14]) for $J_2 < J/2$, observing an exponential decrease as J_{2c} is approached. For $J_2 > J/2$ short-range correlations become incommensurate [8] rendering a reliable determination of $E_0(L = 2n + 1)$ very difficult. Using exact diagonalizations techniques the complete dispersion of the soliton state for odd-length systems can be determined. We have done this at the MG point and a well defined single mode is observable around $q_0 = \pi/2$ [14] with a minimum corresponding to the soliton gap. The soliton s always moves two sites when it moves and hence lives exclusively on one sublattice with the anti-soliton $\bar{s}$ confined to the other. Hence, it is natural to expect a minimum in the dispersion at $q_0 = \pi/2$. Assuming a relativistic dispersion of the soliton, we find for q', the wave-vector closest to q_0:

$$E_{sol}(q') \simeq \Delta_{sol} + \frac{(vq_0)^2}{2\Delta_{sol}}\frac{1}{L^2} + \mathcal{O}(L^{-3}). \tag{3}$$

q' is also the lowest energy state for the odd-length system. Hence, exploiting the finite-size corrections for systems with open boundaries we can determine the soliton velocity, v. At the MG point we find $v/J \simeq 0.43 - 0.45a$.

Perhaps the most interesting question to ask is whether $s\bar{s}$ bound-states form below the continuum. If such bound-states were to form one would expect them to come in triplet-singlet pairs since the soliton and anti-soliton each are $s = 1/2$ particles. Furthermore, if the soliton and anti-soliton interact we would expect a splitting between the associated singlet and triplet, whereas in the absence of any interaction they should be degenerate and both have an energy of precisely $2\Delta_{sol}$. Using spin-inversion to separate the triplet and singlets we have calculated the two gaps for $J_2 < J/2$. The results are shown in Fig. 3 for the MG point. Clearly, the singlet and triplet become degenerate in the thermodynamic limit and performing an extrapolation we find $\Delta_{s=0} = \Delta_{s=1} \simeq 0.2340(1)J = 2\Delta_{sol}$. One find similar results for any $J_2 < J/2$ and we conclude that for these values of J_2 bound-states do not form close to $q = 0, \pi$. However, it remains a possibility that $s\bar{s}$ bound-states form at higher momenta around $q = \pi/2$, where exact bound-states are known [25], or around $q = 0, \pi$ for $J_2 > J/2$ [14]. Thus, the soliton gap, Δ_{sol}, can actually be inferred directly from the triplet gap, $\Delta_{s=1}$, as calculated by White and Affleck [9]. For $J_2 \leq J_{2c}$ the picture is quite different since the system is initially gapless. However, in the presence of a small δ, it is expected from field theoretical arguments that $\Delta_{s=0}/\Delta_{s=1} = \sqrt{3}$ [26,3,27,28] in the limit of $\delta \to 0$ for any $J_2 \leq J_{2c}$.

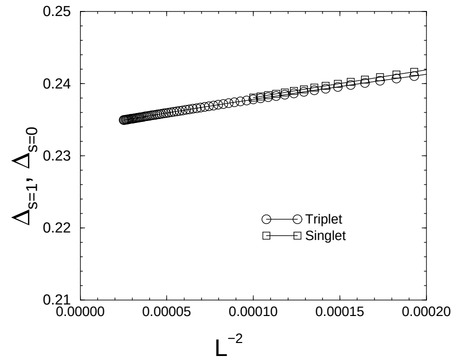

Fig. 3. The triplet, $\Delta_{s=1}$, and singlet, $\Delta_{s=0}$, gaps as a function of L^{-2} at the MG point.

4 Explicitly Dimerized Systems - $s\bar{s}$ Bound States

We next consider systems described by Eq. 2, where an explicit dimerization δ is included. In this case, it has been proposed by one of us [18] that a ladder of triplet-singlet bound-states should occur. The introduction of the explicit dimerization, will favor one of the two otherwise almost degenerate ground-states. The other one being higher in energy of a factor $\sim L\delta$. Hence if the soliton and anti-soliton is separated by only a small distance one can imagine that between them the 'wrong' ground-state is found, and it then seems likely that for small δ a linear potential will be created between the soliton and anti-soliton. This is tentatively indicated in Fig. 4. The lowest

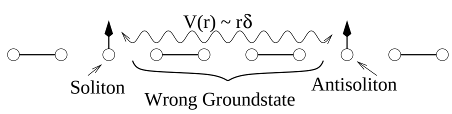

Fig. 4. The creation of a linear potential between a soliton and an anti-soliton.

lying triplet state in the dimerized phase is within this picture best described as a $s\bar{s}$ bound-states and not as a magnon although the difference between the two is largely one of nomenclature. As δ grows the soliton anti-soliton pair becomes tighter and tighter bound and will eventually resemble a single well-defined magnon. The triplet bound-state is always accompanied by a singlet state at a slightly higher energy and at still higher energies a number of other triplet - singlet bound-states appear as indicated in Fig. 5 in the rest-frame of the particle. In the real systems these bound-states can acquire

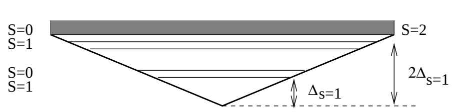

Fig. 5. Singlet and triplet states in the linear potential. The continuum begins at the lowest $S = 2$ state, $E = 2\Delta_{s=1} \sim 4\Delta_{sol}$.

a momentum and disperse. Eventually one reaches energies where it becomes favorable to break up the $s\bar{s}$ bound-state in two lowlying $s\bar{s}$ pairs with energy $2\Delta_{s=1}$. This point constitutes the onset of the $s\bar{s}$-$s\bar{s}$ continuum and can be numerically determined as the lowest lying $S = 2$ state. The natural question to ask is now how many bound-states occur. As δ decreases the linear potential becomes more shallow and can accommodate more bound-states. The continuum, defined as the energy where we can 'pair-produce' will also decrease but not as fast. Hence we expect the number of such bound-state to increase with decreasing δ. At the MG point, Casper and Magnus [25] have found two exact $s\bar{s}$ bound-states, a triplet and singlet both with energy J in our units. One can show that these states remain exact eigenstates along the disorder line, $\delta = 1-2J_2/J$, with energy $(1+\delta)J$ (triplet) and $(1+3\delta)J$ (singlet), and momentum $q = \pi/2$. These states are therefore rather high-lying and could possible form a well-defined single mode at this rather high energy around $q = \pi/2$ even with $\delta = 0$, as suggested by Shastry and Sutherland [15]. It is interesting to note that the splitting between the first triplet and singlet bound-state is always $2\delta J$ along the disorder line at $q = \pi/2$. Numerically, it turns out that this splitting varies only slightly with q. Hence, even at $q = 0$ do we find a splitting close to $2\delta J$. Using DMRG techniques with spin inversion we can follow the lowest lying triplet and singlet states in most of the parameter space. However, to get a complete picture of the dispersion of these bound-states we are limited to exact diagonalization studies in regions where the correlation length is very small in order to limit finite size effects. This is the case along the disorder line and in particular in the vicinity of the MG point. Some of our results are shown in Fig. 7 which clearly show three triplet bound-states and at least two singlet bound-state below the continuum for $J_2 = J/2,\ \delta = 0.05$.

Another important effect is the interaction between impurities and the solitons. A strong impurity will completely break the chains and naively one can model them simply as open chains. The question now becomes if the solitons somehow will bind to the ends of an open chain. In order to investigate this, we imagine an open chain with an odd number of sites and hence a single soliton in the ground-state. At the end of the chain that starts with a weak link a localizing potential will now be created as indicated in Fig. 6. Due to

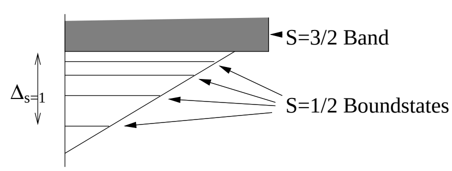

Fig. 6. The potential well created by an open boundary. For the case of an odd site system the continuum will begin at $\Delta_{s=1}$, the lowest state with $S = 3/2$.

the non-zero δ the soliton will bind to the chain-end and a number of $S = 1/2$ soliton-impurity bound-states will be possible in this potential well. As was the case for the $s\bar{s}$ states the soliton-impurity complex can thus be excited into a number of higher lying bound-states before one reaches the continuum defined by the energy where we can excite bulk $s\bar{s}$ states, i. e. $\Delta_{s=1}$. Experimentally transitions between such bound-states can be investigated using Raman, NMR or ESR techniques. Numerically, these bound-states are easily accessible since they are localized. Around the MG point a number of them occur [29].

5 Experimental Evidence

Although several compounds exists that might approximately be described using the simplified Hamiltonians, Eq. 1 and Eq. 2, we shall here concentrate on $CuGeO_3$. Following the initial discovery of a spin-peierls transition in $CuGeO_3$ by Hase et al. [2] a large number of experimental investigations ensued. The experimental situation has been reviewed by Boucher and Regnault [30], and we shall here mainly concentrate on the more recent results of relevance to the presence of soliton bound-states. It is important to realize that couplings to the three-dimensional lattice play an important role in $CuGeO_3$ [31]. These three-dimensional couplings are taken into account in Eq. 2 only at the mean-field level through δ, leading to estimates of J=160 K, $J_2/J = 0.36$, $\delta = 0.014$ [32], and any dynamical effects stemming from phonons are therefore neglected [33]. Inelastic neutron scattering

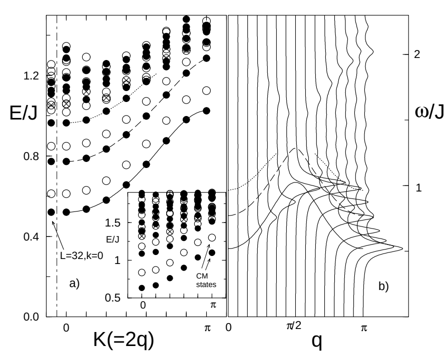

Fig. 7. (**a**) The lowest lying triplet (solid circles), singlets (open circles) and quintuplets (crosses) for $J_2/J = 0.5$, $\delta = 0.05$, $L = 28$, as a function of $k = 2q$. Results for $L = 32$, $k = 0$ are shown to the left. The inset shows the same spectrum from $J_2/J = 0.45$, $\delta = 0.10$, $L = 20$. (**b**) The dynamical structure factor $S^{zz}(q,\omega)$ for $J_2/J = 0.5$, $\delta = 0.05$, $L = 28$ and a broadening of $\varepsilon = 0.04J$. The solid, dashed and dotted lines indicate the 3 triplet branches.

(INS) experiments [34–36] on $CuGeO_3$ have shown rather clear evidence for a well-defined dispersive mode around $q = \pi$, at 2.1meV=16.8cm^{-1}, with a second gap to a continuum. INS is sensitive to triplet excitations and it seems reasonable to interpret this mode as a $s\bar{s}$ triplet bound-state. Additional triplet bound-states seems to be absent in the data. Unfortunately, it is not possible to calculate the number of bound-states at the physical relevant parameters since the correlation length is too big. Secondly, using DMRG techniques we can so far only access the lowest lying singlet and triplet states as well as the continuum at $S = 2$. We therefore study the neighborhood of the MG point ($J_2 = J/2$) where finite-size corrections a very small. With a small dimerization, $\delta = 0.05$, our results are shown in Fig. 7. As shown in the first panel a number of $s\bar{s}$ bound-states clearly occur in agreement with previous results [37]. In the second panel is shown the associated spectral weight. It is interesting to note that the higher lying triplet bound-states yields an almost negligible weight and hence would be difficult to observe experimentally. Secondly, the spectral weight stemming from the $s\bar{s}$ bound-states is concentrated almost exclusively around $q = \pi$ in agreement with the experiments. Even though no clear evidence is seen for higher lying $s\bar{s}$ triplet

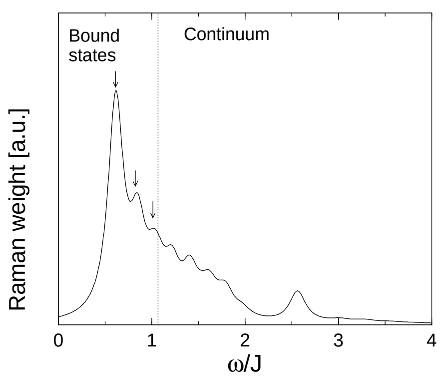

Fig. 8. Raman intensity calculated for a $L = 28$ size system with $J_2/J = 0.5$, $\delta = 0.05$ and a linebroadening $\varepsilon = 0.1J$. The Raman operator $\sum_i \mathbf{S}_i \cdot \mathbf{S}_{i+1}$ was used. The dotted line indicates the lowest lying $S = 2$ state ($L = 28$), indicating the onset of the continuum. The position of the three singlet $s\bar{s}$ bound-states below the continuum are indicated by arrows. See Fig. 7.

bound-states we would expect the accompanying singlet excitations to be visible in inelastic light scattering (ILS) or Raman experiments. This is indeed the case. ILS experiments [38] show very clear evidence for a well defined bound-state around 30 cm^{-1}. We have performed numerical calculations to check that the observed $s\bar{s}$ bound-states in Fig. 7 indeed do yield a sizeable non-zero weight in Raman experiments. Our results are shown in Fig. 8 for a 28 site system with the same parameters as Fig. 7. The singlet $s\bar{s}$ are clearly visible and yield the highest weights. The fact that both a triplet and a singlet bound-state are experimentally observed clearly favors a description in terms of $s\bar{s}$ bound-states. Using NMR techniques it is also possible to study the formation of a soliton lattice in the high field incommensurate phase of $CuGeO_3$ [39].

The formation of soliton-impurity bound-states can also be studied with ILS techniques. Experimentally [40] one observes a line at 15 cm^{-1} in addition to the 30cm^{-1} line present in the pure spectrum. The experiments are in this case performed on $Cu_{1-x}Zn_xGeO_3$. It is reasonable to expect that the only effect of the Zn is to break the chains and introduce open boundaries. Hence, a description in terms of soliton-impurity bound-states as outlined in the previous section should be applicable. Using DMRG techniques it is easy to verify that several such bound-states occur [29,41,20]. The additional line at 15cm^{-1} is interpreted as a transition between *two* soliton-impurity bound-states [40]. The triplet gap is $\Delta_{s=1} = 16.8cm^{-1}$ (see Fig. 6), and the fact that the observed line occurs at energies slightly below this implies that at least *two* $S = 1/2$ bound-states occur. One might expect the number of soliton-impurity bound-states to be related to the number of $s\bar{s}$ bound-states (although in a non-trivial manner), and the experimental observation of two soliton-impurity bound-states could hint at the existence of more $s\bar{s}$ bound-states than the triplet and singlet pair that has been observed so far. Any such additional $s\bar{s}$ bound-states could be very loosely bound and occur close to the continuum making them difficult to detect experimentally.

It is a pleasure to acknowledge discussions with J. Riera and P. Hansen. We thank IDRIS (Orsay) for allocation of CPU time on the C94 and C98 CRAY supercomputers and RS6000 workstations. The research of IA is supported in part by NSERC of Canada.

References

1. L. D. Faddeev and L. A. Takhtajan, Phys. Lett. **85A**, 375 (1981).
2. M. Hase, I. Terasaki, and K. Uchinokura, Phys. Rev. Lett. **70**, 3651 (1993).
3. F. D. M. Haldane, Phys. Rev. B **25**, 4925 (1982).
4. K. Okamoto and K. Nomura, Phys. Lett. A **169**, 433 (1992).
5. S. Eggert, Phys. Rev. B **54**, R9612 (1996).
6. C. K. Majumdar and D. K. Ghosh, J. Math. Phys. **10**, 1399 (1969).
7. U. Schollwöck, Th. Jolicœur, and T. Garel, Phys. Rev. B **53**, 3304 (1996).
8. R. Bursill, G. A. Gehrig, D. J. J. Farnell, J. B. Parkinson, T. Xiang, and C. Zeng, J. Phys. C **7**, 8605 (1995).
9. S. R. White and I. Affleck, phys. Rev. B **54**, 9682 (1996).
10. S. Pati, R. Chitra, D. Sen, H. R. Krishnamurthy, and S. Ramasesha, Euro. Phys. Lett. **33**, 707 (1996).
11. R. Chitra, S. Pati, H. R. Krishnamurthy, D. Sen, and S. Ramasesha, Phys. Rev. B **52**, 6581, (1995).
12. F. Schönfeld, G. Bouzerar, G. S. Uhrig, E. Müller-Hartmann, cond-mat/9803084.
13. K. Maisinger and U. Schollwöck, condmat/9803122.
14. E. Sørensen, I. Affleck, D. Augier and D. Poilblanc, Phys. Rev. B RC cond-mat/9805386.
15. B. Shastry and B. Sutherland, Phys. Rev. Lett **47**, 964 (1981).
16. D. Khomskii, W. Geerstma and M. Mostovoy, Czech. J. of Phys. **46**, Suppl S6, 32 (1996); W. Geerstma and D. Khomskii, Phys. Rev. B **54**, 3011 (1996).
17. J. P. Goff, D. A.Tennant and S. E. Nagler, Phys. Rev. B **52** 15992 (1995).
18. I. Affleck, in *Dynamical properties of Unconventional Magnetic Systems*, ed. A. T. Skjeltorp and D. Sherrington, Kluwer Academic, Dordrecht, Boston (1998).
19. J. Málek, S.-L. Drechsler, G. Paasch, and K. Hallberg, Phys. Rev. B **56**, R8467 (1997).
20. G. S. Uhrig, F. Schönfeld, M. Laukamp, and E. Dagotto, condmat/9805245.

21. T. Nakamura and K. Kubo, Phys. Rev. B **53**, 6393 (1996).
22. D. Sen, B. S. Shastry, R. E. Walstedt, and R. Cava Phys. Rev. B **53**, 6401 (1996).
23. E. Sørensen, to appear in J. Phys. Cond. Matt.
24. S. Ramasesha, Swapan K. Pati, H. R. Krishnamurthy, Z. Shuai and J. L.Brédas, Phys. Rev. B **54**, 7598 (1996).
25. W. J. Caspers and W. Magnus, Phys. Lett. **88A**, 103 (1982).
26. M. C. Cross and D. S. Fisher, Phys. Rev. B **19**, 402 (1979).
27. I. Affleck, Nucl. Phys. B. **265** [FS15], 448 (1986).
28. G. Uhrig and H. Schulz, Phys. Rev. B **54**, R9624 (1996).
29. D. Augier, P. Hansen, D. Poilblanc, J. Riera and E. Sørensen, cond-mat/9807265.
30. J. P. Boucher and L. P. Regnault, J. Phys. I (Paris) **6**, 1939 (1996).
31. G. Uhrig, Phys. Rev. Lett. **79**, 163 (1997).
32. J. Riera and A. Dobry, Phys. Rev. B **51**, 16 098 (1995).
33. D. Augier, D. Poilblanc, E. Sørensen and I. Affleck, Phys. Rev. B **58**, 9110 (1998).
34. M. Arai, M. Fujita, M. Motokawa, J. Akimitsu, and S. M. Bennington, Phys. Rev. Lett. **77**, 3649 (1996).
35. L. P. Regnault, M. Aïn, B. Hennion, G. Dhalenne and A. Revcolevschi Phys. Rev. B **53**, 5579 (1996).
36. M. Aïn, J. E. Lorenzo, G. Dhalenne, A. Revcolevschi, B. Hennion and Th. Jolicœur, Phys. Rev. Lett. **78**, 1560 (1997).
37. G. Bouzerar, A. P. Kampf, and F. Schönfeld, condmat/9701176.
38. P. H. M. van Loosdrecht, J. P. Boucher, G. Martinez, G. Dhalenne, and A. Revcolevschi, Phys. Rev. Lett. **76**, 311 (1996); G. Els, P. H. M. van Loosdrecht, P. Lemmens, H. Vonberg, G. Güntherodt, G. S. Uhrig, O. Fujita, J. Akimitsu, G. Dhalenne, and A. Revcolevschi, Phys. Rev. Lett. **79**, 5138 (1998).
39. Y. Fagot-Revurat, M. Horvatić, C. Berthier, P. Ségransan, G. Dhalenne, and A. Revcolevschi, Phys. Rev. Lett. **77**, 1861 (1996).
40. G. Els, G. S. Uhrig, P. Lemmens, H. Vonberg, P. H. M. van Loosdrecht, G. Güntherodt, O. Fujita, J. Akimitsu, G. Dhalenne, and A. Revcolevschi, cond-mat/9808064.
41. M. Laukamp, G. B. Martins, C. Gazza, A. L. Malvezzi, E. Dagotto, P. M. Hansen, A. C. Lopez and J. Riera, Phys. Rev. B **57**, 1102 (1998).